Local structure of hydrated nanocrystalline films of the proton conductor BaZr<inf>1-x</inf>Sc<inf>x</inf>O<inf>3-x/2</inf> studied by infrared

Vibrational Spectroscopy 130 (2024) 103622

Contents lists available at ScienceDirect

Vibrational Spectroscopy

journal homepage: www.elsevier.com/locate/vibspec

Local structure of hydrated nanocrystalline films of the proton conductor $BaZr_{1-x}Sc_xO_{3-x/2}$ studied by infrared spectroscopy

Elena Naumovska [a], Gabriel Kofi Nzulu [b], Laura Mazzei [a], Arnaud Le Febvrier [b], Kristina Komander [c], Martin Magnuson [b], Max Wolff [c], Per Eklund [b], Maths Karlsson [a,*,1]

[a] Department of Chemistry and Chemical Engineering, Chalmers University of Technology, SE-412 96 Göteborg, Sweden
[b] Department of Physics Chemistry and Biology (IFM), Linköping University, SE-581 83 Linköping, Sweden
[c] Department of Physics and Astronomy, Uppsala University, 75120 Uppsala, Sweden

ARTICLE INFO

Keywords:
Proton conducting oxide
Films
Infrared spectroscopy
Fuel cell
O-H stretch vibration

ABSTRACT

We report results from a study of the local structure of hydrated nanocrystalline 2 μm films of the well known proton conductor $BaZr_{1-x}Sc_xO_{3-x/2}$ with $x = 0.45$, 0.54 and 0.64, using infrared (IR) spectroscopy. The films were prepared by magnetron sputtering. Analysis of the IR spectra focused on the O–H stretching region (2000—3700 cm^{-1}), which reveals the presence of several distinct O–H stretching bands for which the intensity and frequency of each band vary in an unsystematic manner with Sc concentration. The spectra for the two higher Sc concentrations, $x = 0.54$ and 0.64, exhibit a distinct, highly intense O–H stretching band centered at around 3400–3500 cm^{-1}, which is assigned to relatively symmetric, weakly hydrogen-bonding, proton configurations. The spectrum for the lower Sc concentration, $x = 0.45$, does not feature such a band but a broader, weaker, O–H stretching band between approximately 2500 and 3700 cm^{-1}, suggesting that the protons are more homogeneously distributed over a range of different local proton coordinations in this relatively weakly doped material. A comparison to the IR spectra of powder samples of similar compositions suggests that for $x = 0.45$, the spectra and proton coordination of films and powder samples are similar, whereas for $x = 0.54$ and 0.64, a larger fraction of protons seems to be located in weakly hydrogen-bonding proton configurations in the films compared to the respective powder samples.

1. Introduction

Acceptor-doped barium zirconates, such as Sc-doped $BaZrO_3$, typically exhibit high proton conductivities in the intermediate temperature range of 200–500 °C and are, therefore, of high interest to be used as proton conducting electrolytes in next generation, intermediate temperature, solid oxide fuel cells (SOFCs) [1–4]. For applications in miniaturized SOFCs, which are gaining increased attention, the proton conductor has to be in the form of a film [5,6]. In comparison to powder samples, the fabrication of films is very different and films represent a confined state that may be textured, strained, and exhibit varying degrees of crystallinity, which may affect significantly the performance of the electrolyte [7–9]. As one example of the latter, a film of Y-doped $BaZrO_3$ was shown to have two times higher proton conductivity compared to the corresponding powder sample of the same chemical composition [7]. A thorough understanding about the local structure and dynamics of protons in these materials, especially in regard to the difference between films and powder samples, is hence critical to understand the difference in performance of films and powder samples, which is at present not fully understood.

In this work, using IR spectroscopy, we investigate the local structure of nanocrystalline films of Sc-doped $BaZrO_3$ (Sc/BZO) as fabricated by magnetron sputtering. Previous local structural investigations of Sc/BZO have primarily focused on powder samples of $BaZr_{1-x}Sc_xO_{3-x/2}$ with the Sc dopant concentration (x) ranging from 0.1 to 0.6, which show that Sc/BZO exhibits an average cubic structure (space group $Pm\bar{3}m$), however with local deviations of the average cubic structure increasing as a function of Sc dopant concentration [10–18]. In comparison, studies of proton conducting perovskites in the form of (thin) films have focused on epitaxial films of the Y-doped system $BaZr_{1-x}Y_xO_{3-x/2}$, which showed that grain-boundaries have a negative impact on proton conductivity [2,7]. Here, we focus on the Sc-doped system

* Corresponding author.
E-mail address: maths.karlsson@chalmers.se (M. Karlsson).
[1] ORCID: 0000-0002-2914-6332

https://doi.org/10.1016/j.vibspec.2023.103622
Received 19 September 2023; Received in revised form 13 November 2023; Accepted 21 November 2023
Available online 24 November 2023

with three different Sc dopant concentrations, *i.e.* $BaZr_{1-x}Sc_xO_{3-x/2}$ with $x = 0.45$, 0.54 and 0.64. The aim of the study is to get information about the local coordination of protons, how it depends on the Sc dopant concentration and, notably, how it compares to the much more studied powder samples.

2. Experimental

2.1. Sample preparations

The films, about 2 μm in thickness, of $BaZr_{1-x}Sc_xO_{3-x/2}$ with $x = 0.45$, 0.54, and 0.64, were grown on 1 mm thick double-side polished c-plane Al_2O_3 substrates, by magnetron co-sputtering using three different targets with $BaZrO_3$ as the main source, Sc as dopant and Ba for balance of the metallic ratio, *i.e.* (Ba/(Zr+Sc)) = 1. Details of the preparation and structural analysis of the films are reported in ref. [19]. For each composition, three identical films were prepared, and hydrated samples were prepared by annealing one film for each composition. The annealing was achieved by heat treatment in a tube furnace subjected to a nitrogen flow with water vapor, while cooling from 600 °C to 200 °C at a rate of 0.2 °C/min. Dry samples were prepared by heating one film for each composition to 400 °C, followed by cooling to 200 °C at a rate of 50 °C/min. The degree of hydration for each of the samples was determined by nuclear reaction analysis (NRA), which shows that the hydration degrees of the films varies from 28% for $x = 0.45$, through 22% for $x = 0.54$, and to 19% for $x = 0.64$. Details about the NRA measurements on the films can be found in the Supporting Information (SI).

2.2. Infrared spectroscopy measurements

IR spectroscopy measurements were performed over the frequency range of 450–5000 cm^{-1}, using a Thermo Scientific Nicolet Nexus IR spectrometer. However, due to strong absorption in the lower-frequency part of the spectra, we only analyze the 1900–5000 cm^{-1} region which covers the region of O–H stretching modes in proton conducting oxides [17,20,21]. The measurements on films were performed in transmission mode. Reference spectra for all films were acquired by taking measurements on a 1 mm thick sample of double-side polished Al_2O_3 film, which is fully transparent in the investigated frequency range of 450–5000 cm^{-1}. IR absorbance-like spectra were derived by taking the logarithm ratio between the reference and sample spectra and this was done automatically by the software Thermo Scientific OMNIC FTIR [22]. All measurements were performed at room temperature in air. Due to unwanted interference caused by the thickness of the substrate, the IR spectra of all sample were smoothed using the Savitzky-Golay algorithm in the Thermo Scientific OMNIC FTIR software [22]. Examples of the non-smoothed raw data on films are shown in the SI.

3. Results and discussion

Fig. 1 shows the IR absorbance spectra of the $BaZr_{1-x}Sc_xO_{3-x/2}$ with $x = 0.45$, 0.54, and 0.64 samples, in both the dehydrated and hydrated forms. For the dehydrated samples [Fig. 1(a)], we observe that the spectra have an oscillatory-like behavior across the whole spectral range of 1900–5000 cm^{-1}. While we are unable to reproduce these oscillations by a simple wave function, such as a sinus wave, these oscillations are likely to be the result of interference from multiple internal reflections within the substrate. However, since the substrates are expected to be identical, the fact that the spectra are different for the different samples may point towards slight but significant differences in the thickness, and structure, of the films.

Upon hydration, the spectra of all three materials change significantly, also as a function of Sc dopant level [Fig. 1(b)]. For the two higher Sc dopant concentrations, $x = 0.54$ and $x = 0.64$, we observe that the oscillation peaking at around 2700 cm^{-1} is now broadened, but most noticeable is the appearance of a relatively intense band at around

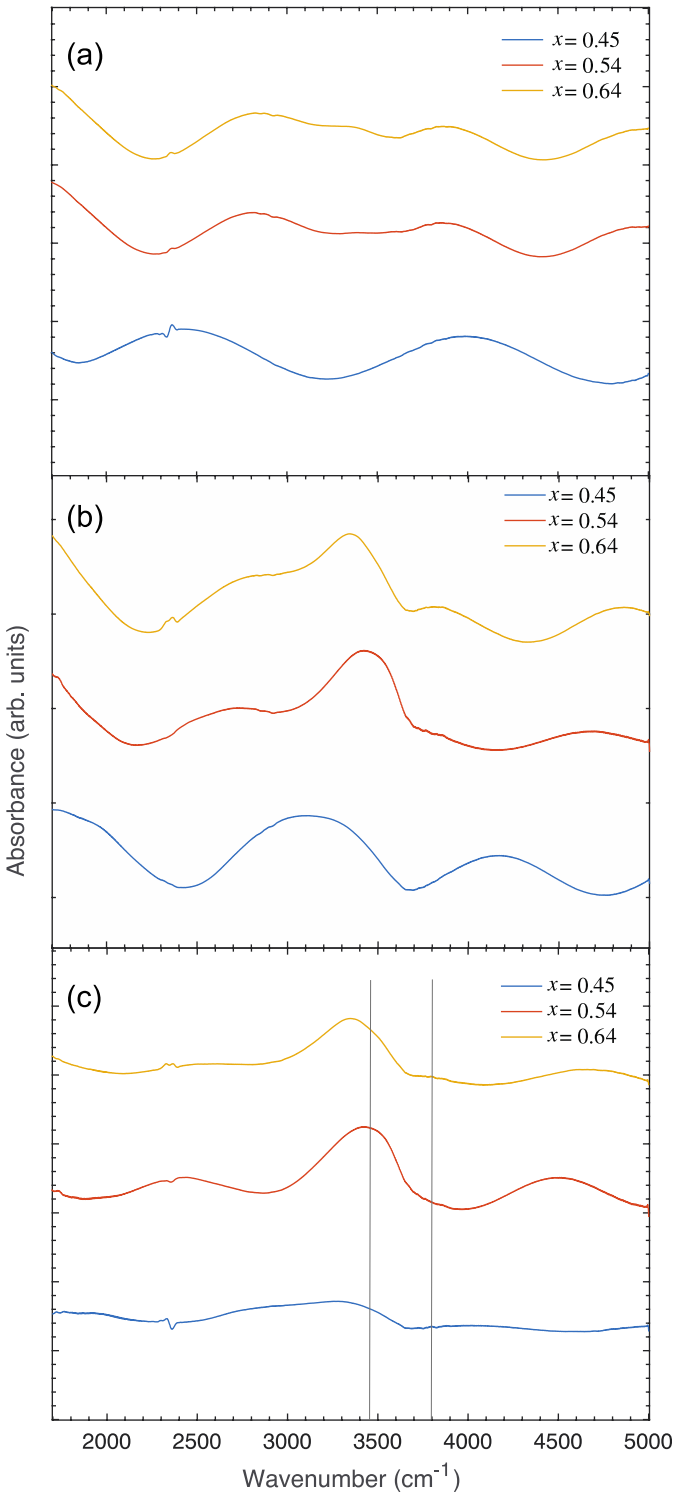

Fig. 1. IR spectra of the films of $BaZr_{1-x}Sc_xO_{3-x/2}$ where $x = 0.45$, 0.54, and 0.64. a) dehydrated and b) hydrated films, and c) subtracted spectra of hydrated and dehydrated films. The spectra have been vertically offset for clarity. The two vertical lines mark out the positions for the distinct 3450 cm^{-1} and weak 3800 cm^{-1} bands for $x = 0.54$ (see main text).

3400 cm^{-1}, whereas for $x = 0.45$ we do not observe this band. One should note, because of the generally weak bands, also after hydration, it is most likely that also the hydrated spectra are significantly affected by the interference of the underlying substrate and/or due to the films themselves. To derive spectra virtually free, or at least with such interference effects strongly suppressed, we plot in Fig. 1(c) the difference

spectra between the hydrated and dehydrated films.

As can be seen, the difference spectra are manifested by a much weaker oscillatory nature, suggesting that our analysis is robust. Crucially, Fig. 1(c) reveals several differences between the different materials. For $x = 0.45$, the spectrum is characterized by a broad, weak band between 2500 and 3700 cm^{-1}, with no other significant features. For $x = 0.54$, the spectrum is characterized by a very distinct band at around 3450 cm^{-1} and a weak feature at around 3800 cm^{-1}. For $x = 0.64$, the spectrum is similar to the one for $x = 0.54$, but the 3450 cm^{-1} band is now down-shifted to about 3300 cm^{-1}. The other features in the spectra for $x = 0.54$ and $x = 0.64$ are ascribed to oscillations related to interference in the films.

For comparison, Fig. 2 shows literature data of the IR spectra of fully hydrated powder samples of $BaZr_{1-x}Sc_xO_{3-x/2}$ with $x = 0.10$ and 0.50, as adapted from Mazzei *et al.* [18]. As can be seen, the IR spectra of the two powder samples are similar, despite the large difference in Sc dopant levels. Specifically, the spectra are dominated by a large O–H stretching band between 2500 and 3700 cm^{-1}, and an O–H stretching + wagging combination band at around 4250 cm^{-1}, and, generally, the intensity of all bands increases with increasing Sc dopant level [18]. In more detail, the broad nature of the O–H stretching band between 2500 and 3700 cm^{-1} is the result of a range of different local proton environments in the materials, where the lower-frequency part (2500–3000 cm^{-1}) is assigned to protons in relatively non-symmetrical environments, such as Zr-OH-Sc and Zr-OH-Sc vacancy, and the higher-frequency part (3000–3700 cm^{-1}) is assigned to protons in relatively symmetrical environments, such as Zr-OH-Zr and Sc-OH-Sc [18,21]. The lower frequency of O–H stretching modes in non-symmetrical proton configurations is due to an increased tendency for the formation of hydrogen bonds between the protons and neighboring oxygens of the perovskite lattice [18,21,23]. Such hydrogen bonding leads to an increase of the O–H bond length and a decreased O–H stretching frequency. Likewise, protons in symmetrical environments are featured by weak or no hydrogen bonding to neighboring oxygens. Therefore, the generally broad nature of the O–H stretching band for the two powder samples manifests a wide distribution of hydrogen-bond strengths between the protons and neighboring oxygens of the perovskite lattice, as a result of a wide range of different local proton configurations. Note, some of the cited literature above is on In-doped $BaZrO_3$, and assignments are based on the assumption that Sc behaves similar to In as dopant atom in $BaZrO_3$ based proton conductors, which is a reasonable assumption considering their similar ionic radii and local structural deformation upon doping as seen in previous studies using vibrational spectroscopy [18,23].

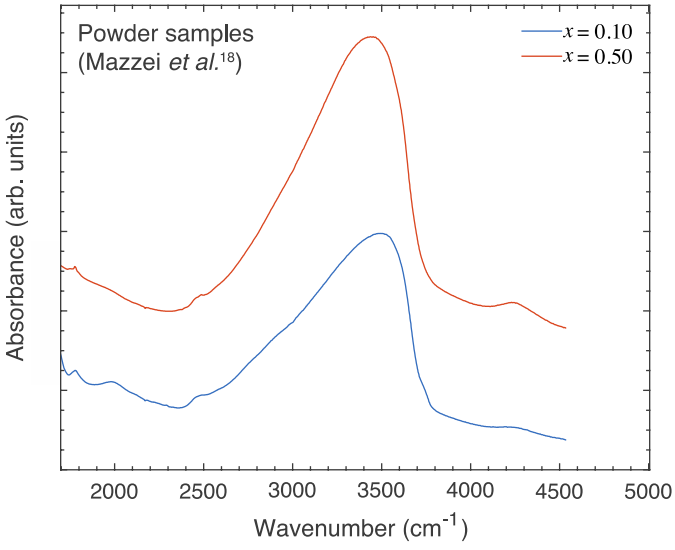

Fig. 2. IR absorbance spectra of hydrated powder samples of $BaZr_{1-x}Sc_xO_{3-x/2}$ with $x = 0.10$, and 0.50.
Adapted from Ref. [18].

By combining the results from the analysis of IR spectra of nanocrystalline films and powder samples, we observe several important features, *cf.* Figs. 1(c) and 2. In particular, we note the quite inhomogeneous O–H stretching band profile for the films and, in particular, the presence of a distinct, highly intense band centered at around 3400–3700 cm^{-1} for the two higher Sc dopant concentrations ($x = 0.54$ and 0.64). This suggests that the proton site distribution is less homogenous in the nanocrystalline films for $x = 0.54$ and 0.64, with a larger fraction of protons in relatively symmetric, weakly hydrogen bonding configurations, as compared to the $x = 0.45$ film and to the powder samples. Thus, while the nanocrystalline film for $x = 0.54$ and the powder samples for all Sc dopant levels as investigated here are generally characterized by a wide range of proton sites, with no obvious preferred local proton configurations, the nanocrystalline films for $x = 0.54$ and 0.64 are featured by a preferred, weakly hydrogen-bonded, proton site. Based on the IR data, a compositional threshold for the creation of such a preferred proton site may lay between $x = 0.45$ and $x = 0.54$, above which the spectra are relatively similar. Since the nanostructure, *i.e.* the average particle distribution, does not change significantly as a function of Sc dopant level [24], this threshold is likely to be associated with a change in the local structural details of the material. A comparison to powder samples of cubic-structured barium zirconate based proton conductors suggests that an increase of dopant concentration normally leads to increased local structural distortions in the perovskite lattice, as can be ascribed to tilts of the octahedral moieties [25]. Therefore, above a certain threshold composition between $x = 0.45$ and $x = 0.54$, the local structural distortions may have reached a certain level to create a unique local proton configuration, featured by weak hydrogen-bonding interactions, which appears to be only present in the films.

The observation of a different behavior for the $x = 0.45$ film with respect to the $x = 0.54$ and 0.64 films is highly interesting, yet it is difficult to explain and we prefer to not be too speculative in this matter. However, we note that an increase in Sc dopant concentration in combination with stresses in the films, possibly due to the lattice-mismatch to the Al_2O_3 substrate, or due to the nature of the film deposition itself, may contribute to localized pronounced tilts of the octahedral moieties of the perovskite lattice, which may create unique, preferred, proton configurations with weak hydrogen bonding in the films with $x = 0.54$ and 0.64. The difference in local structure between films with different Sc concentrations, and between films and powder samples, may as well be linked to the degree of hydration of the respective materials. We note that, for the films, the degree of hydration decreases systematically with increasing Sc concentration, whereas for the powder samples, both samples were reported to be fully hydrated [18]. This may indicate that dopant-induced local structural distortions may not, *per se*, make the materials more difficult to hydrate, at least not under the hydration conditions as used in this study. Rather, we speculate that dopant induced stresses in the films, possibly accelerated due to some lattice-mismatch to the Al_2O_3 substrate, give rise to local structures that are associated to the unique O–H stretching band profile and may as well be related to the films' generally lower degree of hydration.

4. Conclusions

Our IR spectroscopy study of magnetron-sputtered films of the proton conducting perovskites $BaZr_{1-x}Sc_xO_{3-x/2}$ with $x = 0.45$, 0.54, and 0.64 reveals the presence of several distinct bands related to O–H stretching vibrations and for which the intensity and frequency of each bandvary in an unsystematic manner with Sc dopant concentration. In particular, the IR spectra for the two higher Sc dopant concentrations exhibit a distinct, highly intense band centered at relatively high vibrational frequency, 3400–3500 cm^{-1}, which is a signature of that

most protons are located in relatively symmetric, weakly hydrogen bonding, configurations. This is considerably different from the corresponding powder samples, which exhibit a broad O–H stretching band, between 2500 and 3700 cm^{-1}, as a result of a wide and relatively smooth distribution of hydrogen-bond strengths to the protons in the material. That is, the local coordination of protons seems to be less homogenous in the nanocrystalline films, as compared to the powder samples.

Declaration of Competing Interest

The authors declare that they have no known competing financial interests or personal relationships that could have appeared to influence the work reported in this paper.

Data availability

Data will be made available on request.

Acknowledgments

We thank the Swedish Government Strategic Research Area in Materials Science on Functional Materials at Linköping University (Faculty Grant SFO-Mat-LiU No. 2009 00971), the Knut and Alice Wallenberg Foundation through the Wallenberg Academy Fellows program (P. E. Grant No. 2020.0196), the Swedish Energy Agency through Grants No. 43606-1 (M. M.) and 48712-1 (M. K., P. E., A. le F.) M. M. also acknowledges support from the Carl Trygger Foundation (CTS20:272, CTS16:303, CTS14:310). Infrastructure grants by VR-RFI (Grant Nos. 2017-00646-9, 2019-00191) and SSF (contract RIF14-0053) supporting the operation of the accelerator at the Tandem Laboratory in Uppsala are gratefully acknowledged.

Appendix A. Supporting information

Supplementary data associated with this article can be found in the online version at doi:10.1016/j.vibspec.2023.103622.

References

[1] C. Duan, J. Tong, M. Shang, S. Nikodemski, M. Sanders, S. Ricote, A. Almansoori, R. O'Hayre, Readily processed protonic ceramic fuel cells with high performance at low temperatures, Science 349 (2015) 1321–1326.
[2] K. Bae, D.Y. Jang, H.J. Choi, D. Kim, J. Hong, B.K. Kim, J.H. Lee, J.W. Son, J. H. Shim, Demonstrating the potential of yttrium-doped barium zirconate electrolyte for high-performance fuel cells, Nat. Commun. 8 (2017), 14553.
[3] S. Choi, C.J. Kucharczyk, Y. Liang, X. Zhang, I. Takeuchi, H.I. Ji, S.M. Haile, Exceptional power density and stability at intermediate temperatures in protonic ceramic fuel cells, Nat. Energy 3 (2018) 202–210.
[4] Y. Chen, B. deGlee, Y. Tang, Z. Wang, B. Zhao, Y. Wei, L. Zhang, S. You, K. Pei, J. H. Kim, Y. Ding, P. Hu, F.F. Tao, M. Liu, A robust fuel cell operated on nearly dry methane at 500 °C enabled by synergistic thermal catalysis and electrocatalysis, Nat. Energy 3 (2018) 1042–1050.
[5] B.C. Steele, A. Heinzel, Materials for fuel-cell technologies, Nature 414 (2001) 345–352.
[6] E. Traversa, Toward the miniaturization of solid oxide fuel cells, Electrochem. Soc. Interface 18 (2009) 49.
[7] D. Pergolesi, E. Fabbri, A. D'Epifanio, E. Di Bartolomeo, A. Tebano, S. Sanna, S. Licoccia, G. Balestrino, E. Traversa, High proton conduction in grain-boundary-free yttrium-doped barium zirconate films grown by pulsed laser deposition, Nat. Mater. 9 (2010) 846–852.
[8] Y.B. Kim, T.M. Gür, H.J. Jung, S. Kang, R. Sinclair, F.B. Prinz, Effect of crystallinity on proton conductivity in yttrium-doped barium zirconate thin films, Solid State Ion. 198 (2011) 39–46.
[9] T. Higuchi, T. Owaku, Y. Iida, E. Sakai, M. Kobayashi, H. Kumigashira, Proton conduction of $BaCe_{0.90}Y_{0.10}O_{3-\delta}$ thin film with lattice distortion, Solid State Ion. 270 (2015) 1–5.
[10] I. Ahmed, M. Karlsson, S.G. Eriksson, E. Ahlberg, C.S. Knee, K. Larsson, A.K. Azad, A. Matic, L. Börjesson, Crystal structure and proton conductivity of $BaZr_{0.9}Sc_{0.1}O_{3-\delta}$, J. Am. Ceram. Soc. 91 (2008) 3039–3044.
[11] K.D. Kreuer, W. Münch, A. Fuchs, U. Klock, J. Maier, Proton conducting alkaline earth zirconates and titanates for high drain electrochemical applications, Solid State Ion. 145 (2001) 295–306.
[12] J. Hyodo, K. Kitabayashi, K. Hoshino, Y. Okuyama, Y. Yamazaki, Fast and stable proton conduction in heavily scandium-doped polycrystalline barium zirconate at intermediate temperatures, Adv. Energy Mater. 10 (2020), 2000213.
[13] I. Oikawa, H. Takamura, Correlation among oxygen vacancies, protonic defects, and the acceptor dopant in Sc-doped $BaZrO_3$ studied by ^{45}Sc nuclear magnetic resonance, Chem. Mater. 27 (2015) 6660–6667.
[14] H. Takahashi, I. Oikawa, H. Takamura, Atomistic insight into the correlation among oxygen vacancies, protonic defects, and the acceptor dopants in Sc-Doped $BaZrO_3$ using first-principles calculations, J. Phys. Chem. C 122 (2018) 6501–6507.
[15] A.L. Buzlukov, I.Y. Arapova, S.V. Verkhovskii, I.A. Leonidov, O.N. Leonidova, A. P. Gerashenko, A.P. Stepanov, V.L. Kozhevnikov, Hydrogen dynamics features in $BaZr_{1-x}Sc_xO_{3-x/2}(OH)_y$: high-temperature ^{1} H NMR studies, J. Solid State Electrochem. 20 (2016) 609–617.
[16] L. Buannic, L. Sperrin, R. Dervişoğlu, F. Blanc, C.P. Grey, Proton distribution in Sc-doped $BaZrO_3$: a solid state NMR and first principle calculations analysis, Phys. Chem. Chem. Phys. 20 (2018) 4317–4328.
[17] M. Karlsson, I. Ahmed, A. Matic, S.G. Eriksson, Short-range structure of proton-conducting $BaM_{0.10}Zr_{0.90}O_{2.95}$ (M= Y, In, Sc and Ga) investigated with vibrational spectroscopy, Solid State Ion. 181 (2010) 126–129.
[18] L. Mazzei, A. Perrichon, A. Mancini, L. Malavasi, S.F. Parker, L. Börjesson, M. Karlsson, Local coordination of protons in In-and Sc-doped $BaZrO_3$, J. Phys. Chem. C 123 (2019) 26065–26072.
[19] G.K. Nzulu, E. Naumovska, M. Karlsson, P. Eklund, M. Magnuson, A. le Febvrier, Growth and thermal stability of Sc-doped $BaZrO_3$ thin films deposited on single crystal substrates, Thin Solid Films 772 (2023), 139803.
[20] K.D. Kreuer, Aspects of the formation and mobility of protonic charge carriers and the stability of perovskite-type oxides, Solid State Ion. 125 (1999) 285–302.
[21] M. Karlsson, M.E. Björketun, P.G. Sundell, A. Matic, G. Wahnström, D. Engberg, L. Börjesson, I. Ahmed, S.G. Eriksson, P. Berastegui, Vibrational properties of protons in hydrated $BaIn_xZr_{1-x}O_{3-x/2}$, Phys. Rev. B 72 (9) (2005), 094303.
[22] B. Zimmermann, A. Kohler, Optimizing Savitzky–Golay parameters for improving spectral resolution and quantification in infrared spectroscopy, Appl. Spectrosc. 67 (2013) 892–902.
[23] L. Mazzei, A. Perrichon, A. Mancini, G. Wahnström, L. Malavasi, S.F. Parker, L. Börjesson, M. Karlsson, Local structure and vibrational dynamics in indium-doped barium zirconate, J. Mater. Chem. A 7 (2019) 7360–7372.
[24] C.Y. Regalado Vera, H. Ding, J. Urban-Klaehn, M. Li, Z. Zhao, F. Stewart, H. Tian, X. Liu, Y. Dong, J. Li, M. Zhou, H. Luo, D. Ding, Improving proton conductivity by navigating proton trapping in high scandium-doped barium zirconate electrolytes, Chem. Mater. 35 (2023) 5341–5352.
[25] Z. Lin, S. Lin, Y. Tian, A. Van Bokkelen, M. Valerio, M.A. Gomez, Oxygen vacancies altering the trapping in the proton conduction landscape of doped barium zirconate, J. Phys. Chem. C 124 (2020) 27954–27964.